Supplementary Materials for

Molecular Control of δ-Opioid Receptor Signaling

Gustavo Fenalti[1*], Patrick M. Giguere[2*], Vsevolod Katritch[1], Xi-Ping Huang[2], Aaron A. Thompson[1], Vadim Cherezov[1], Bryan L. Roth[2#], Raymond C. Stevens[1#]

Affiliations:

[1]Department of Integrative Structural and Computational Biology, The Scripps Research Institute, 10550 North Torrey Pines Road, La Jolla, CA 92037, USA

[2]National Institute of Mental Health Psychoactive Drug Screening Program and Department of Pharmacology and Division of Chemical Biology and Medicinal Chemistry, University of North Carolina Chapel Hill Medical School, Chapel Hill, NC 27599, USA

***** Contributed equally

[#]To whom correspondence should be addressed: bryan_roth@med.unc.edu or stevens@scripps.edu

Keywords: human opioid receptor, sodium regulation, allostery, functional selectivity, GPCR signaling, constitutive activity, arrestin

Supplementary Tables

Table S1: Data collection and refinement statistics.

Structure	***BRIL-δOR(ΔN/ΔC)-naltrindole***
Data Collection	(APS GM/CA CAT 23ID-D, 20 μm beam)
Number of crystals	47
Space group	$C2_1$
Cell dimensions	
a, *b*, *c* (Å)	86.23, 72.85, 84.41
α, β, γ (°)	90.0, 107.4, 90.0
Number of reflections measured	204,142
Number of unique reflections	45,488
Resolution (Å)[a]	40.0-1.80 (1.86-1.80)
R_{merge} (%)	10.4 (82.2)
Mean $I/\sigma I$	16.4 (2.3)
Completeness	98.5 (98.5)
Redundancy	4.5 (4.3)
Refinement	
Resolution	29.7-1.80
Number of reflection (test set)	43,157 (2,303)
R_{work}/R_{free} (%)	17.1/19.0
Number of atoms	
Protein	3,140
Naltrindole	31
Sodium ion	1
Lipids and other	410
Overall B values (Å^2)	
δOR(ΔN/ΔC)	34.3
BRIL	49.8
Naltrindole	26.2
Na+	26.6
Lipids and other	60.9
rmsd	
Bond lengths (Å)	0.012
Bond angles (°)	1.4
Ramachandran plot statistics (%)[b]	
Most favoured regions	99.5
Additionally allowed regions	0.5
Disallowed regions	0

$R_{merge} = \Sigma_{hkl} | I(hkl) - < I(hkl) > | / \Sigma_{hkl}(hkl)$, where < I(hkl) > is the mean of the symmetry equivalent reflections of I(hkl). [a]Highest resolution shell is shown in parentheses. [b]As defined in MolProbity.

***Table S2*: Summary of metal binding site calculations to validate the sodium ion presence in the allosteric site of δ-OR.** Calculations were performed using the CMM server http://csgid.org/csgid/metal_sites/ which uses well established concepts for ion validation[1-5].

Metal	**Occupancy***	**B factor§**	**Valence¶ [2]**	**nVECSUM# [1]**	**R.M.S.D. (°)****
Na^+	1	26.6 (26.9)	1.0	0.082	16.5
Li^+	1	2.0 (27.2)	0.3	0.19	21.1
K^+	1	37.4 (26.5)	2.4	0.071	16.6

*Occupancy for atom under consideration.
§ Metal ion B factor with valence-weighted; environmental average B factor in parenthesis.
¶Summation of bond valence values for an ion binding site. Valence accounts for metal-ligand distances.
#Summation of ligand vectors weighted by bond valence values and normalized by overall valence; values increase when the coordination sphere is not symmetrical due to incompleteness.
**R.M.S. deviation of observed geometry angles compared to ideal geometry (in degrees).

Table S3: **Analysis of the effects of sodium ions on the binding of δ-OR ligands.** Displacement of [^{3}H] Naltrindole in the absence and presence (140 mM) of sodium chloride from WT δ-OR expressed in HEK293 cells, and the crystallized construct BRIL-δOR(ΔN/ΔC)-naltrindole expressed in *Sf*9 insect cells. Data were analyzed using a one-site model. Values represented as pK_i average ± SEM (Ki nM) from minimum of two assays, each in triplicate.

Ligand type and name		**HEK 293 WT δ-OR pK_i ± SEM (K_i, nM)**		***Sf*9 BRIL-δOR(ΔN/ΔC) pK_i ± SEM (K_i, nM)**	
		0 NaCl	**140mM NaCl**	**0 NaCl**	**140mM NaCl**
Small molecule	**(-) Bremazocine**	7.46 ± 0.06 (35)	7.33 ± 0.05 (47)	7.88 ± 0.11 (13)	7.84 ± 0.12 (14)
	(-) Cyclazocine	7.01 ± 0.07 (97)	6.81 ± 0.07 (155)	7.11 ± 0.07 (78)	6.94 ± 0.07 (114)
	Diprenorphine	7.88 ± 0.06 (13)	7.63 ± 0.06 (24)	7.51 ± 0.06 (31)	7.46 ± 0.07 (35)
	Etorphine	7.06 ± 0.08 (88)	6.21 ± 0.08 (613)	6.22 ± 0.07 (601)	5.84 ± 0.07 (1569)
	Naltrindole	9.05 ± 0.07 (0.9)	9.21 ± 0.06 (0.6)	8.94 ± 0.05 (1.2)	9.11 ± 0.04 (0.8)
Peptide	**DADLE**	6.56 ± 0.11 (280)	5.58 ± 0.11 (2600)	5.92 ± 0.07 (1200)	5.23 ± 0.07 (5900)

Table S4: **Effects of various δ-OR mutations on Gα_i and β-arrestin activity.** δ-ORs WT and mutants where assayed for **Gα_i** -signaling and β-arrestin-recruitment as described in the Methods section. Data were subjected to non-linear least-squares regression analysis using the sigmoidal dose-response function. Data of four independent experiments (N=4) performed in quadruplicate are presented. Representative data are show in **Fig. 4**. β-arrestin and G protein activation are presented as % of BW373U86 ± SEM, EC_{50} (nM) and $LogEC_{50}$ ± SEM. "No activation" indicated that no activation was observed or the sigmoidal curve was not convergent or ambiguous.

δ-OR mutants	**Ligands**	**β-arrestin activation Emax (% of BW373U86 ± SEM)**	**β-arrestin activation EC_{50} (nM)**	**β-arrestin activation $LogEC_{50}$ ± SEM**	**$G\alpha_i$ activation E_{max} (% of BW373U86 ± SEM)**	**$G\alpha_i$ activation EC_{50} (nM)**	**$G\alpha_i$ activation $LogEC_{50}$ ± SEM**
WT	Naltrindole	no activation	no activation	no activation	**53.4 ± 2.8**	**21.9**	**-7.66 ± 0.10**
	Naltriben	no activation	no activation	no activation	**28.8 ± 2.0**	**19.5**	**-7.70 ± 0.14**
	BNTX	no activation	no activation	no activation	no activation	no activation	no activation
	BW373U86	**99.8 ± 1.7**	**3.9**	**-8.41 ± 0.04**	**100.0 ± 1.5**	**3.6**	**-8.44 ± 0.03**
	DADLE	**42.4 ± 0.9**	**0.83**	**-9.08 ± 0.05**	**102.2 ± 1.3**	**1.3**	**-8.90 ± 0.03**
	Deltorphin II	**38.6 ± 1.1**	**2.0**	**-8.69 ± 0.08**	**104.9 ± 3.2**	**1.5**	**-8.82 ± 0.06**
D95A	Naltrindole	**64.3 ± 1.0**	**4.2**	**-8.37 ± 0.03**	no activation	no activation	no activation
	Naltriben	**65.3 ± 1.3**	**5.6**	**-8.25 ± 0.04**	**24.8 ± 2.5**	**30.3**	**-7.51 ± 0.10**
	BNTX	**59.9 ± 3.1**	**66.5**	**-7.17 ± 0.08**	no activation	no activation	no activation
	BW373U86	**99.3 ± 2.4**	**30.7**	**-7.51 ± 0.04**	**98.4 ± 2.7**	**21.9**	**-7.66 ± 0.04**
	DADLE	**39.5 ± 1.6**	**58.0**	**- 7.23 ± 0.07**	**77.0 ± 3.3**	**15.6**	**-7.80 ± 0.08**
	Deltorphin II	**43.7 ± 2.8**	**105.7**	**-6.97 ± 0.09**	**75.4 ± 2.7**	**1.5**	**-8.83 ± 0.07**
N310A	Naltrindole	**45.0 ± 1.0**	**50.0**	**-7.30 ± 0.03**	no activation	no activation	no activation
	Naltriben	**44.6 ± 1.8**	**69.1**	**-7.16 ± 0.06**	no activation	no activation	no activation
	BNTX	**48.9 ± 3.3**	**646.4**	**-6.18 ± 0.07**	no activation	no activation	no activation
	BW373U86	**101.8 ± 4.0**	**192.7**	**-6.71 ± 0.06**	**100.7 ± 8.7**	**10.1**	**-7.99 ± 0.18**
	DADLE	no activation	no activation	no activation	no activation	no activation	no activation
	Deltorphin II	no activation	no activation	no activation	no activation	no activation	no activation
N314A	Naltrindole	**25.5 ± 1.4**	**36.7**	**-7.43 ± 0.09**	no activation	no activation	no activation
	Naltriben	**27.1 ± 3.0**	**70.0**	**-7.15 ± 0.19**	no activation	no activation	no activation
	BNTX	no activation	no activation	no activation	no activation	no activation	no activation

	BW373U86	**75.2 ± 5.3**	**77.2**	**-7.11 ± 0.11**	**99.9 ± 2.7**	**13.8**	**-7.86 ± 0.05**
	DADLE	no activation	no activation	no activation	**78.6 ± 4.5**	**52.3**	**-7.28 ± 0.08**
	Deltorphin II	no activation	no activation	no activation	**89.5 ± 5.7**	**0.5**	**-9.26 ± 0.2**
N131A	Naltrindole	no activation	no activation	no activation	no activation	no activation	no activation
	Naltriben	no activation	no activation	no activation	no activation	no activation	no activation
	BNTX	no activation	no activation	no activation	no activation	no activation	no activation
	BW373U86	no activation	no activation	no activation	no activation	no activation	no activation
	DADLE	no activation	no activation	no activation	no activation	no activation	no activation
	Deltorphin II	no activation	no activation	no activation	no activation	no activation	no activation
N131V	Naltrindole	no activation	no activation	no activation	no activation	no activation	no activation
	Naltriben	no activation	no activation	no activation	no activation	no activation	no activation
	BNTX	no activation	no activation	no activation	no activation	no activation	no activation
	BW373U86	no activation	no activation	no activation	**120.3 ± 6.2**	**27.9**	**-7.55 ± 0.11**
	DADLE	no activation	no activation	no activation	**100.0 ± 4.9**	**4.4**	**-8.35 ± 0.10**
	Deltorphin II	no activation	no activation	no activation	**35.8 ± 3.4**	**3.1**	**-8.51 ± 0.16**

Table S5*. Effects of various mutations on δ-OR radioligand binding parameters.** For these experiments ^{3}H-naltrindole saturation and DADLE competition assays using ^{3}H-Naltrindole in the absence of sodium chloride were performed. Results are presented as average ± SEM from two or more separate experiments, each in triplicate. Binding curves were fit to a one-site model. The same data were also fit to a two-site model and the results are shown in ***Table S6. NA=no activity; these receptor mutants expressed receptor which did not bind ^{3}H-naltrindole.

δ-OR	**^{3}H-naltrindole K_d (nM)**	**DADLE binding affinity against ^{3}H-naltrindole**		
		[^{3}H-naltrindole] nM in assays	**pK_i ± SEM (n)**	**Average K_i (μM)**
Wild-type	0.52	1.25 – 1.60	6.47 ± 0.09 (4)	0.34
D95A	0.68	1.25 – 1.60	5.51 ± 0.04 (5)	3.09
D95N	0.96	1.25 – 1.60	5.45 ± 0.05 (5)	3.52
D128A	NA	NA	NA	NA
N131A	1.17	1.25 – 1.60	7.12 ± 0.06 (5)	0.08
N131V	1.17	1.25 – 1.60	6.83 ± 0.06 (5)	0.15
S135A	NA	NA	NA	NA
N310A	NA	NA	NA	NA
N314A	NA	NA	NA	NA

Table S6. **DADLE binding against ^{3}H-Naltrindole in the absence of sodium chloride fit to a two-site model.** Results are presented as average ± SEM from three or four assays. High affinity fraction values were taken directly from curve-fitting. High and low IC_{50} values and their corresponding 95% Confidence Intervals (C.I.) were taken from curve-fitting and converted to corresponding high and low affinity (pK_i) and 95% C.I. values using the Cheng-Prusoff equation. Note that Asp95Ala reduced high DADLE binding affinity, but did not significantly reduce the high affinity fraction. Asp95Asn reduced the high affinity fraction, but did not reduce DADLE high affinity. Asn131Ala or Asn131Val increased DADLE high affinity. DADLE low affinity remained unchanged in all mutants.

δ-OR	**High affinity fraction**	**High pK_i (95% C.I.)**	**Low pK_i (95% C.I.)**
Wild-type	0.70 ± 0.05	6.90 (7.06 – 6.73)	5.10 (5.48 – 4.72)
D95A	0.49 ± 0.19	6.07 (6.55 – 5.59)*	4.95 (5.42 – 4.49)
D95N	0.17 ± 0.05**	6.72 (7.32 – 6.11)	5.14 (5.26 – 5.04)
N131A	0.69 ± 0.12	7.46 (7.59 – 7.34)*	4.57 (4.85 – 4.29)
N131V	0.75 ± 0.03	7.24 (7.35 – 7.13)*	4.81 (5.15 – 4.47)

* $P < 0.0001$ and ** $p < 0.05$ as compared with WT δ-OR.

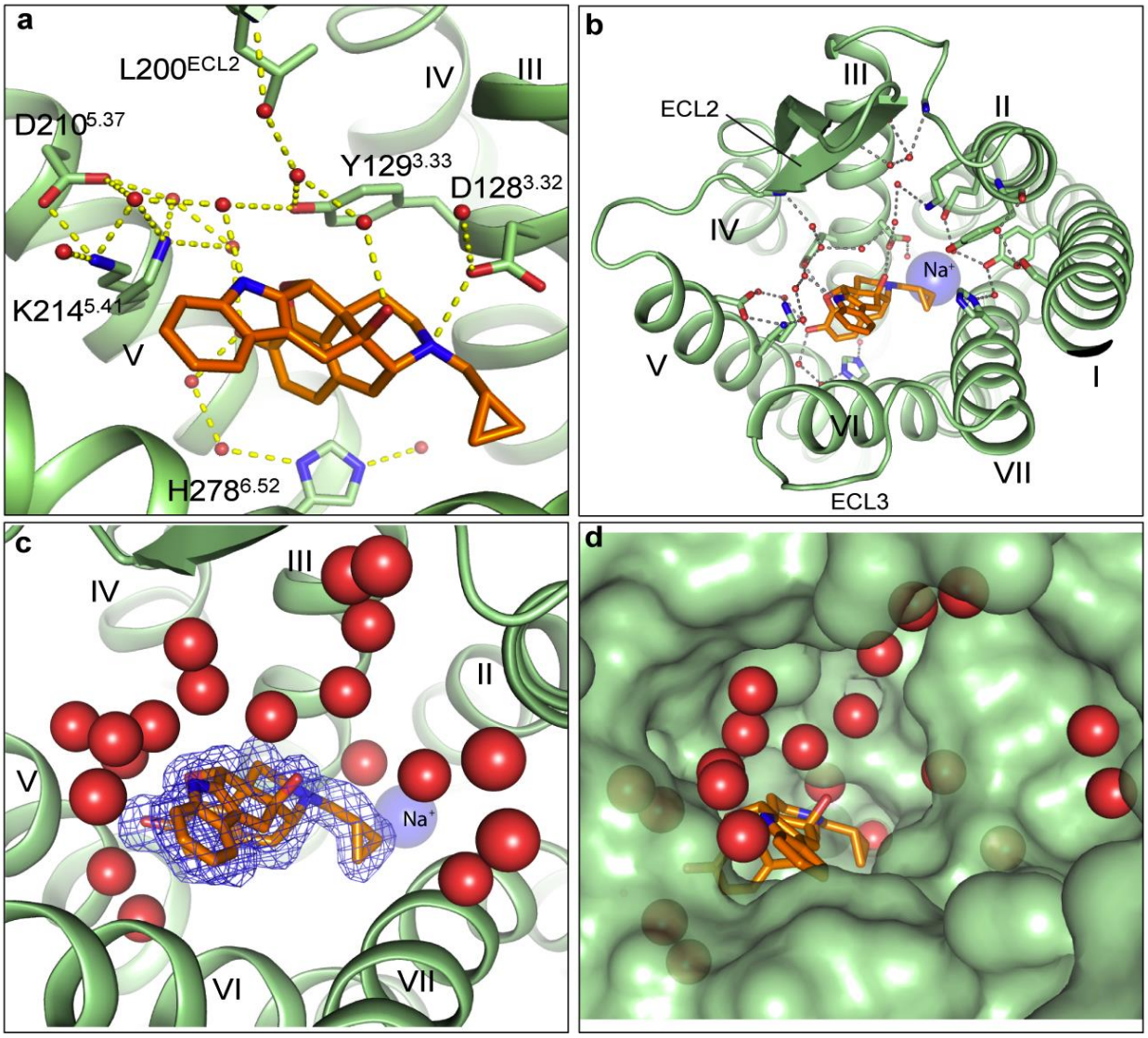

***Fig. S1*. Interactions in the orthosteric ligand binding site of BRIL-δOR(ΔN/ΔC)-naltrindole.** (**a**) 'Close up' view of the hydrogen bond interaction network (yellow dotted lines) between the ligand naltrindole (orange sticks) and receptor (green cartoon; side chains shown as sticks) showing water (red spheres) mediated interactions. (**b**) Overview of water mediated interactions (grey dotted lines) in the orthosteric pocket of BRIL-δOR(ΔN/ΔC)-naltrindole. (**c**) mF_o- DF_c "omit" electron density map (blue mesh) around naltrindole (orange sticks) after simulated annealing in PHENIX[6] (5000K; contoured at 3σ); all water molecules surrounding the ligand in the orthosteric site are shown (red spheres). (**d**) Surface representation of the BRIL-δOR(ΔN/ΔC)-naltrindole (green surface) showing the position of naltrindole (orange sticks) and the water cluster (red spheres) in the orthosteric site.

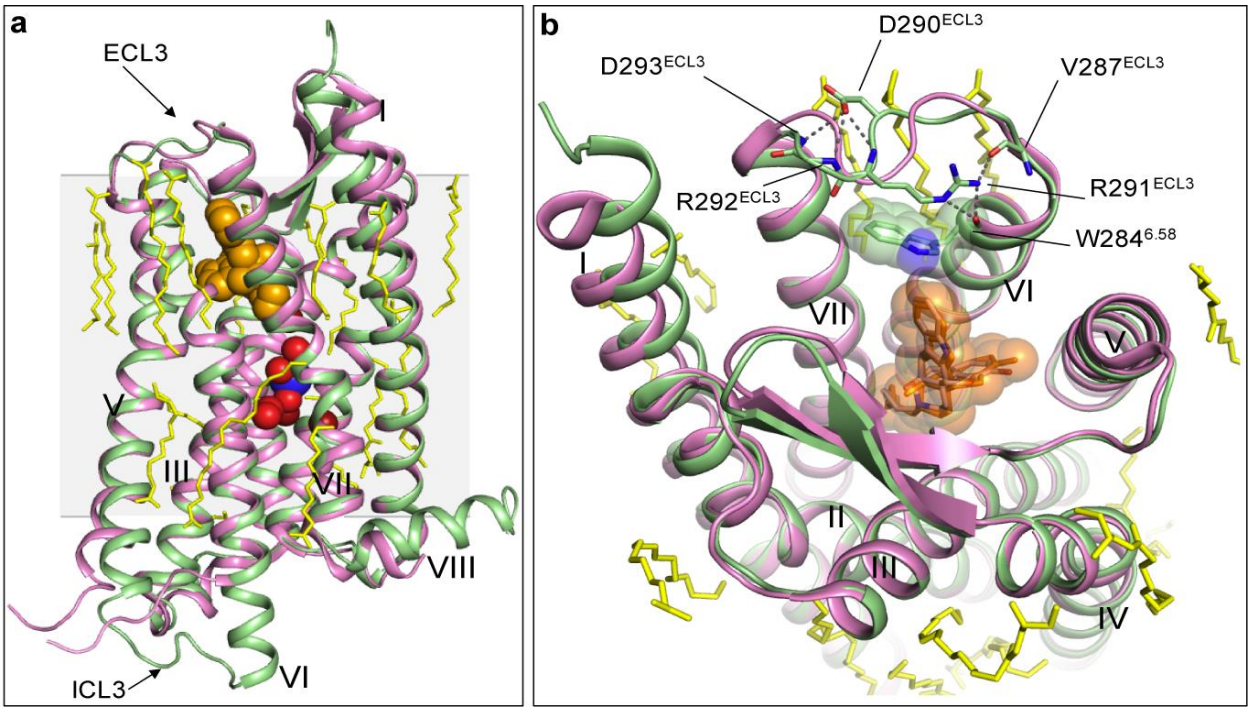

Fig. S2. **Superposition of *Mus musculus* and human δ-OR receptor structures.** (**a**) Comparison of the human BRIL-δOR(ΔN/ΔC)-naltrindole structure (green) with the previously determined 3.4 Å crystal structure of the *Mus musculus* δOR-T4L (magenta; PDB ID 4EJ4). The ligand naltrindole in the BRIL-δOR(ΔN/ΔC)-naltrindole structure is shown as orange spheres and is omitted in the 4EJ4 structure. Water molecules and the sodium ion in the allosteric site of BRIL-δOR(ΔN/ΔC)-naltrindole structure are shown as red and blue spheres respectively. The grey box represents the approximate regions of the receptor 7TM domain embedded in the lipidic bilayer; yellow sticks represent lipids. ICL3 fusion protein in 4EJ4 (T4L) and N-terminal BRIL fusion protein in BRIL-δOR(ΔN/ΔC)-naltrindole structures are omitted. (**b**) ECL3 conformation of human δ-OR and comparison with mouse δOR-T4L ECL3 structure. BRIL-δOR(ΔN/ΔC)-naltrindole is shown as green cartoon and side chains are depicted as green sticks. The ligand naltrindole is represented by orange carbon sticks and transparent spheres (BRIL-δOR(ΔN/ΔC)-naltrindole structure) and magenta carbon sticks (4EJ4 structure).

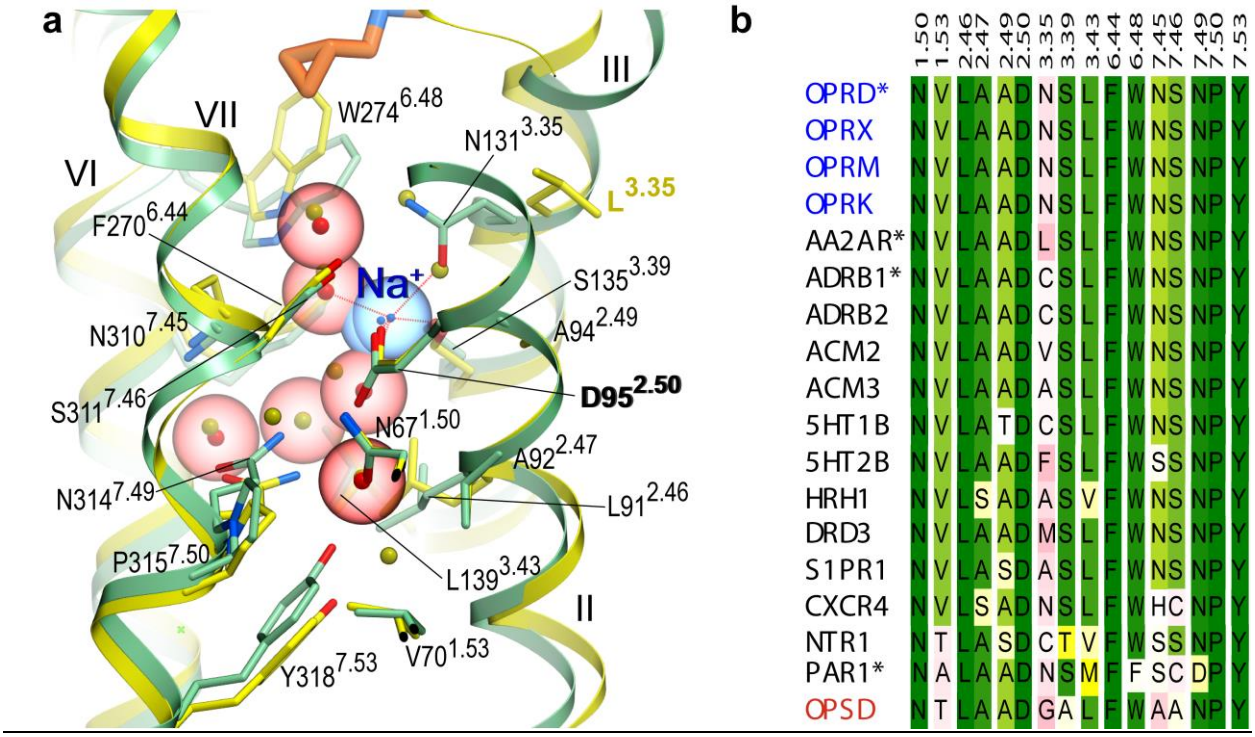

Fig. S3. **Conservation of the allosteric pocket in class A GPCRs harboring a sodium ion and a water cluster.** (**a**) Structural comparison of the sodium pocket between BRIL-δOR(ΔN/ΔC)-naltrindole structure (green cartoon and carbon atoms) and sodium-bound 1.8 Å resolution structure of adenosine A_{2A} receptor[6] (A_{2A}AR; PDB ID 4EIY; yellow cartoon and carbons). Water molecules of the pocket in δ-OR structure are shown by red transparent spheres and smaller solid spheres, while water molecules in A_{2A}AR structure pocket are shown with small yellow solid spheres only. Sodium ions in both structures are shown with blue transparent spheres, with red dotted lines from Na^+ to the five coordinating oxygen atoms shown in the δ-OR structure. Part of the ligand naltrindole is shown as thick sticks with orange carbons. The comparison reveals identical side chains and similar conformations in 15 residue positions of the pocket (numbered as in δ-OR, with superscripts showing Ballesteros-Weinstein positions of the residues[7]). The important exception is 3.35 position that in δ-OR features a polar Asn131$^{3.35}$ side chain coordinating the Na^+ ion, while in A_{2A}AR the Leu87$^{3.35}$ side chain is oriented towards the lipidic membrane. (**b**) Sequence comparison of the allosteric sodium pocket residues in currently available crystal structures of class A GPCRs. Asterisk marks receptors with high-resolution crystallographic evidence for sodium ions coordinated by the D$^{2.50}$ side chain. Note that Rhodopsin (OPSD) lacks polar residues in key positions 3.39, 7.45 and 7.46, which sets it apart from other class A receptors.

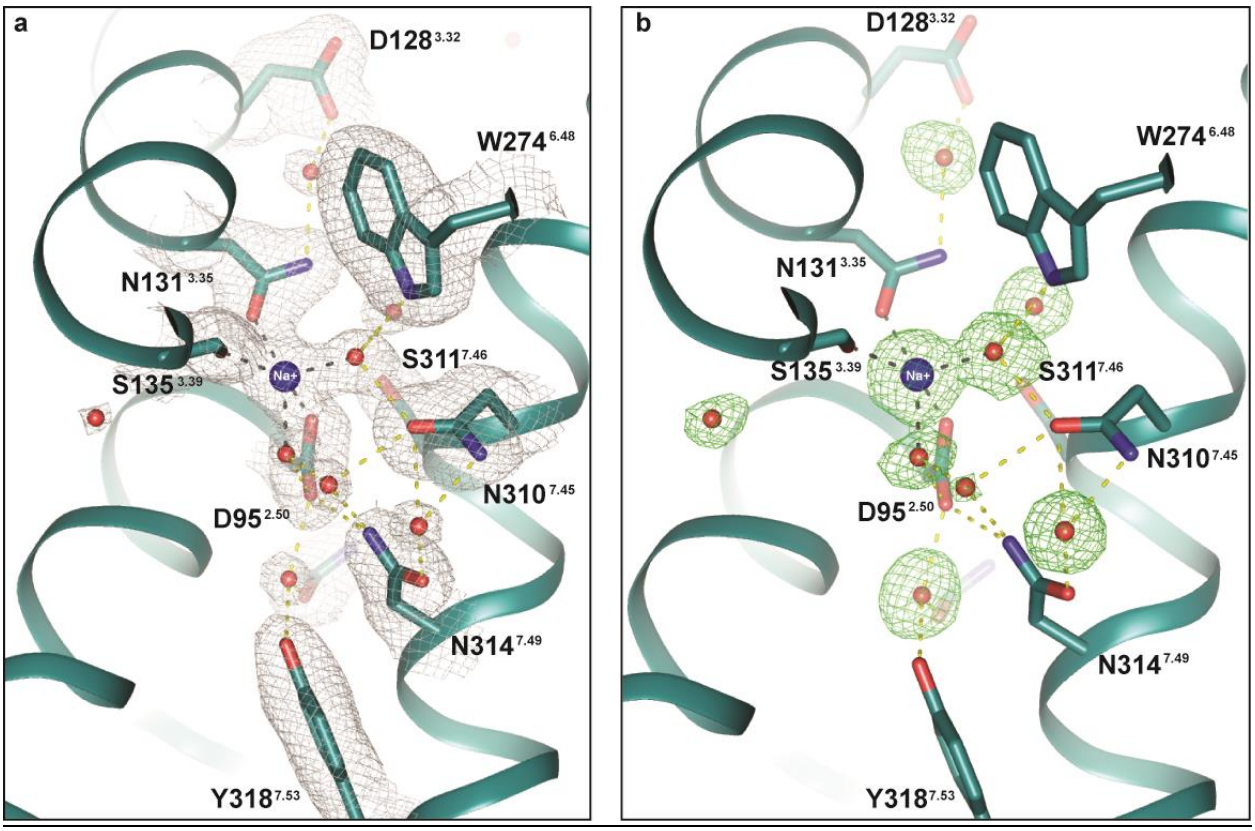

Fig. S4. **Electron density maps around the δ-OR sodium binding site.** (**a**) 2mF_o- DF_c electron density map (grey mesh) of receptor residues (cyan sticks) around the sodium ion (blue sphere) binding site contoured at 1σ. Black dashed lines represent interactions between the sodium ion and the atoms in direct contact with the receptor residues or water molecules in the first hydration shell of the ion. Yellow dashed lines shows the hydrogen bond network of water molecules and receptor residues. These polar interactions in the core of the 7TM bundle of the receptor establish an axis of connectivity between the orthosteric binding site, allosteric sodium site and residues in the intracellular side of the receptor. (**b**) mF_o- DF_c "omit" electron density map of sodium ion and coordinating water molecules after simulated annealing in PHENIX[8] (5000K; contoured at 3σ).

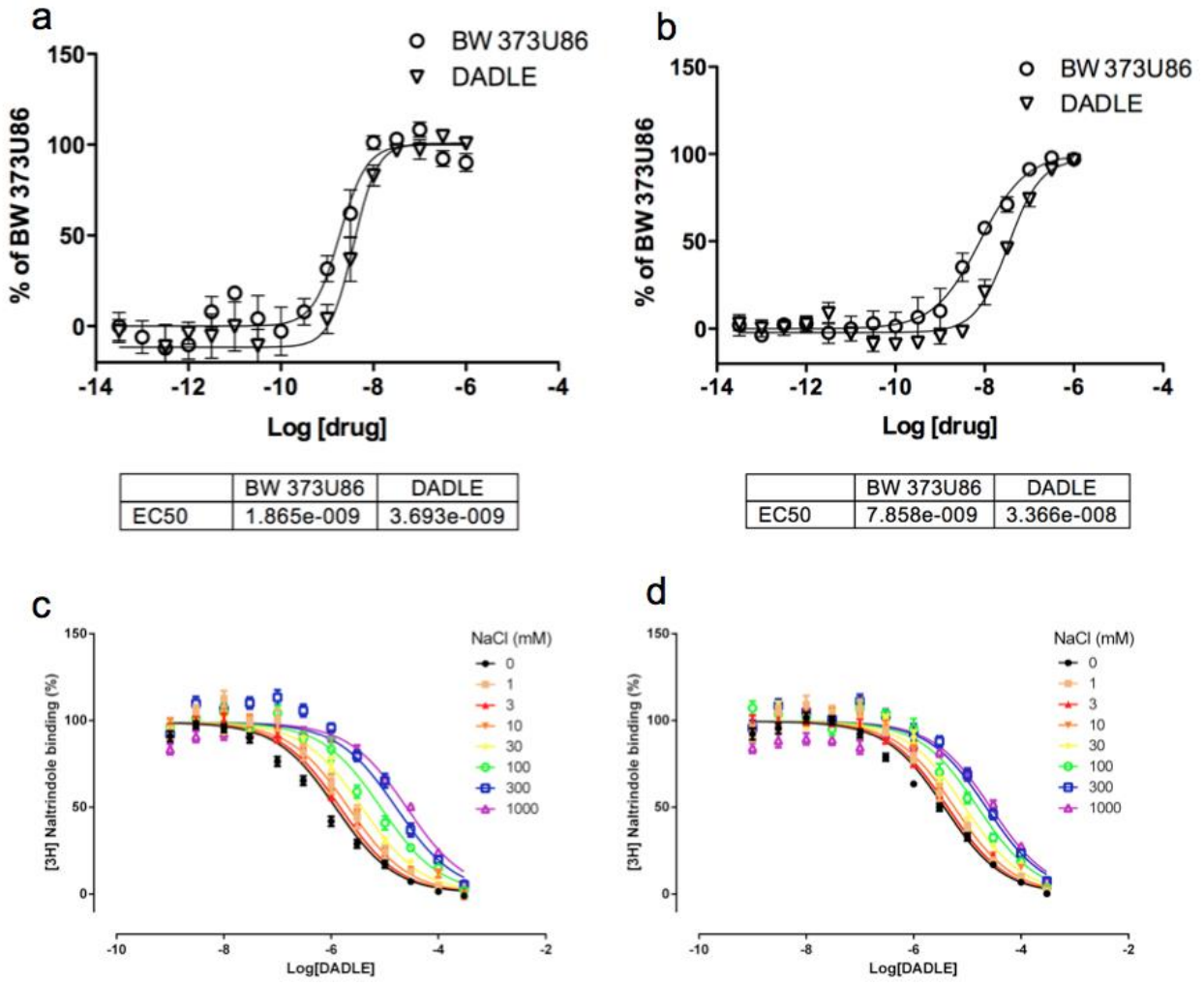

	BW 373U86	DADLE
EC50	1.865e-009	3.693e-009

	BW 373U86	DADLE
EC50	7.858e-009	3.366e-008

Fig. S5. **Functional characterization of WT δ-OR and the engineered BRIL-δOR(ΔN/ΔC) construct used for crystallization.** G-protein signaling characterization for (**a**) WT and (**b**) BRIL-δOR(ΔN/ΔC) is shown. Allosteric inhibitory effect of sodium on DADLE binding to ^{3}H-naltrindole labeled (**c**) WT δ-OR expressed in HEK293 cells (positive control) and (**d**) the BRIL-δOR(ΔN/ΔC) construct used for crystallization and expressed in *Sf*9 cells. Ligand binding data in (**d**) were analyzed using the allosteric model, and the results are shown in **Table 1**. Data represent the mean of four independent experiments each in quadruplicate.

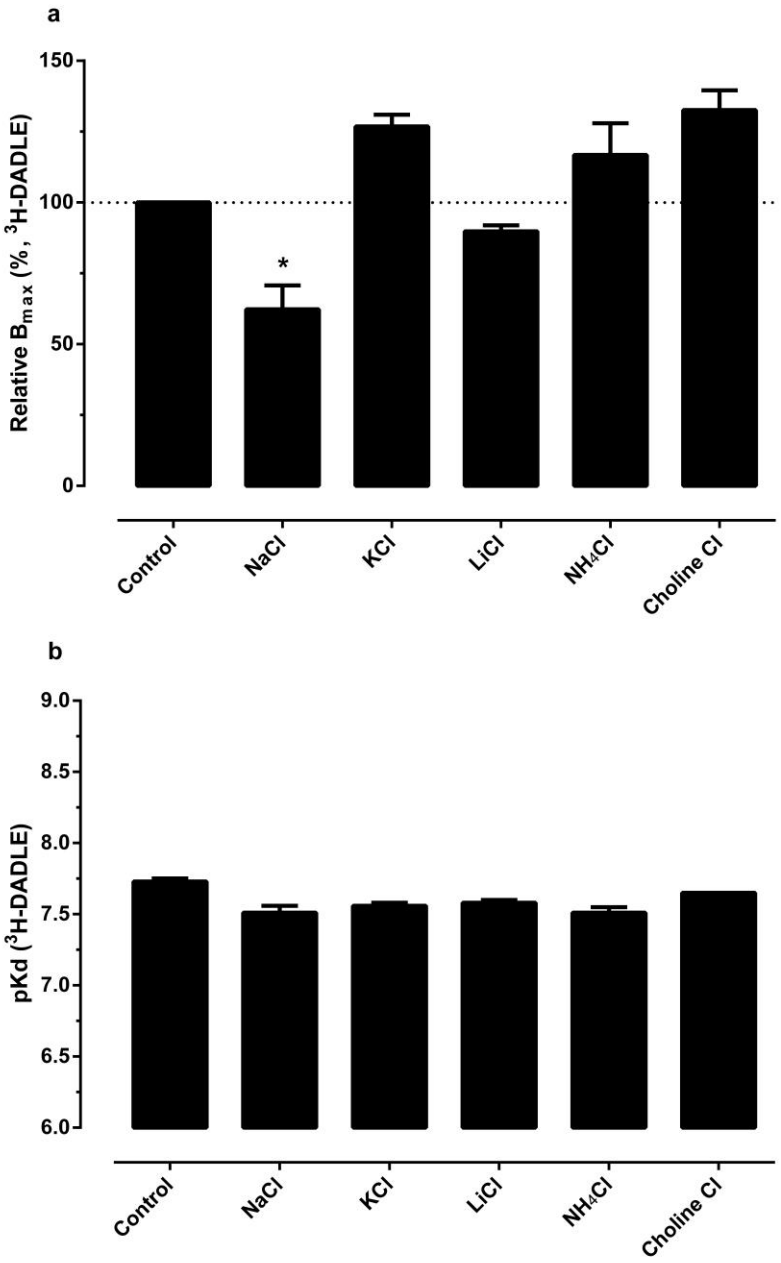

Fig. S6. **Effects of different monovalent cations on the binding of DADLE to BRIL-δOR(ΔN/ΔC).** The effects of different cations on both the total number of binding sites (relative B_{max} in Panel a) and affinity (pK_d in Panel b) of ^{3}H-DADLE at the crystallized δ-OR construct expressed in *Sf*9 cells. ^{3}H-DADLE saturation binding assays were conducted with control binding buffer (50 mM Tris HCl, pH 7.40) in the absence (control) and presence of 100 mM of the indicated chloride salts. Results were analyzed in Prism to obtain B_{max} and K_d values. The B_{max} values were then normalized to control (100%) in each assay. Values represent mean ± SEM from 3 independent assays, each in triplicate. Note: *$p<0.05$ by one-way ANOVA.

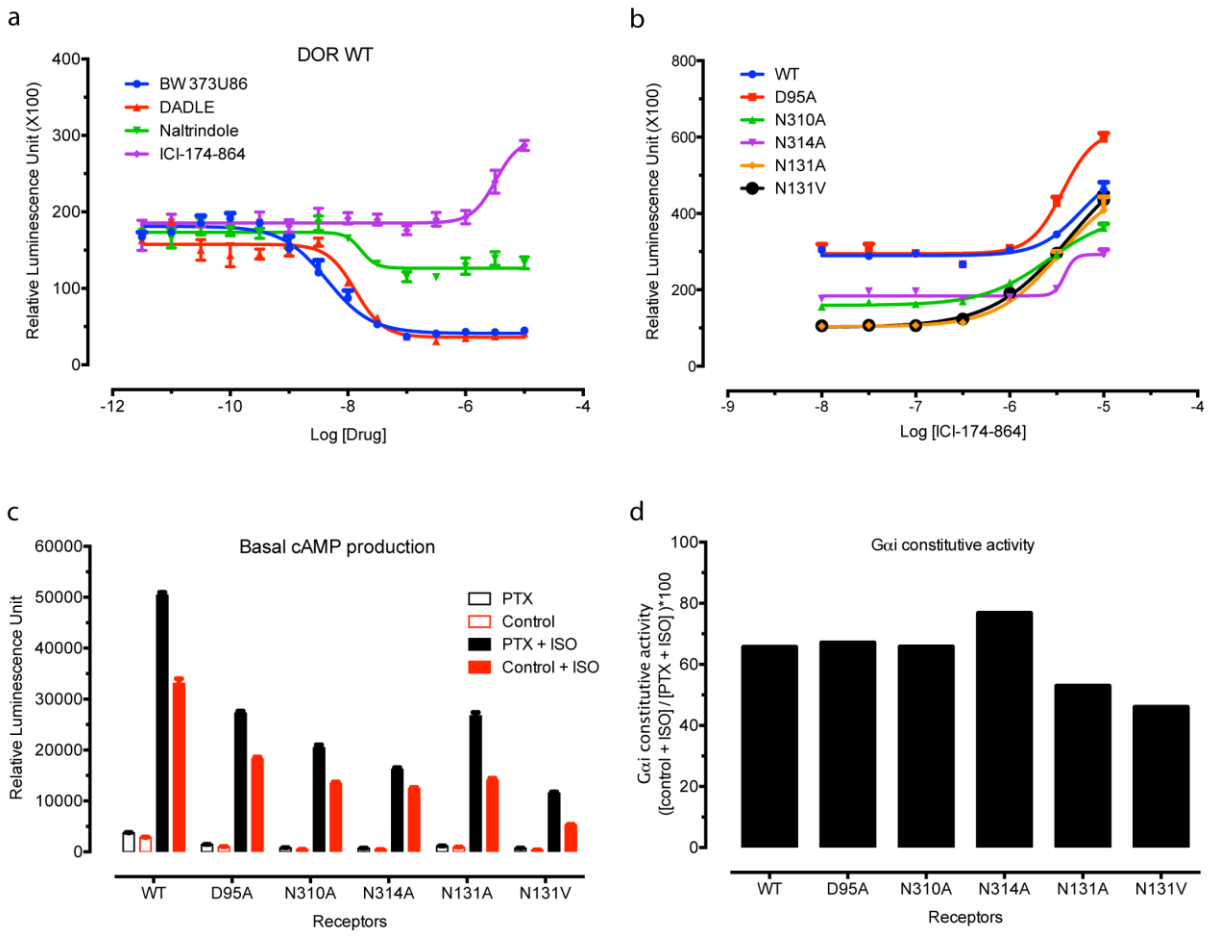

Fig. S7. **Effect of sodium site mutations on basal Gα_i activity**. HEK293 cells were transfected with 10 µg of receptor DNA and 10 µg of Glosensor per 15-cm dish and WT and mutant δ-ORs were assayed for Gα_i-signaling as described in the Methods section. (**a**) Concentration-responses of WT δ-OR-mediated Gα_i signaling induced by the agonists BW 373U86 and DADLE, the antagonist* Naltrindole, and the inverse agonist ICI-174-864. (**b**) Concentration-responses of δ-OR WT and mutants-mediated Gα_i signaling induced by the inverse agonist ICI-174-864. (**c-d**) Cells were treated with 100 ng/ml PTX for 12 hours, depleting all Gα_i constitutive activity. (**c**) Non-normalized basal cAMP level of the δ-OR WT and mutants in the presence or absence of the pertussis toxin (PTX) and isoproterenol (ISO). (**d**) Net Gα_i -constitutive activity was calculated using formula: cAMP level (RLU) from control + ISO / cAMP level (RLU) from PTX + ISO * 100. The data in (**a**) and (**b**) represent the mean ± S.E.M. of at least four different experiments each in quadruplicate. The data in (**c**) and (**d**) represent the mean ± S.E.M of 32 wells (N=32).

* Weak partial agonist activity of Naltrindole at Gα_i signaling was previously described[9,10].

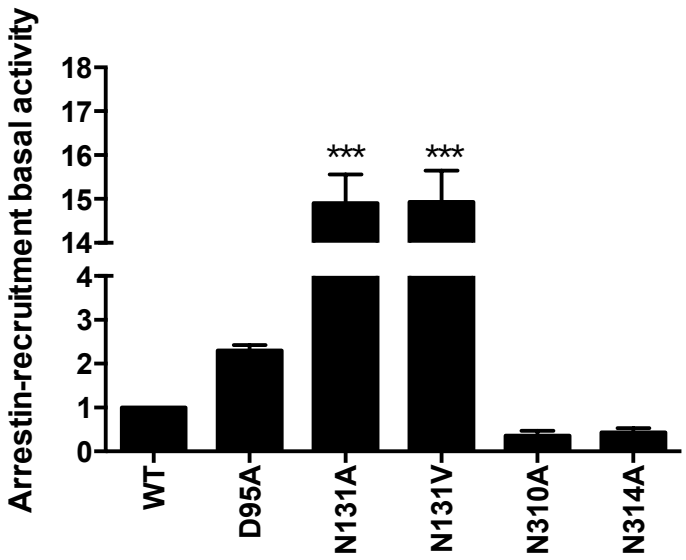

Fig. S8. **Effect of sodium site mutations on basal β-arrestin signaling**. WT and mutant δ-ORs were assayed for β-arrestin-recruitment as described in the Methods section. HTLA cells were transfected with 15 μg of receptor DNA per 15-cm dish and basal activity measured 48 h later. Data are presented relative to WT receptor using the means ± S.E.M. of at least four different experiments each in quadruplicate; *$p<0.05$, **$p<0.01$ and ***$p<0.001$ by one-way ANOVA.

References

1 Muller, P., Kopke, S. & Sheldrick, G. M. Is the bond-valence method able to identify metal atoms in protein structures? *Acta Crystallogr. D* **59**, 32-37 (2003).

2 Brown, I. D. Recent developments in the methods and applications of the bond valence model. *Chem Rev* **109**, 6858-6919, doi:10.1021/cr900053k (2009).

3 Zheng, H., Chruszcz, M., Lasota, P., Lebioda, L. & Minor, W. Data mining of metal ion environments present in protein structures. *J Inorg Biochem* **102**, 1765-1776, doi:10.1016/j.jinorgbio.2008.05.006 (2008).

4 Nayal, M. & Di Cera, E. Valence screening of water in protein crystals reveals potential Na+ binding sites. *J Mol Biol* **256**, 228-234 (1996).

5 Kuppuraj, G., Dudev, M. & Lim, C. Factors governing metal-ligand distances and coordination geometries of metal complexes. *J Phys Chem B* **113**, 2952-2960, doi:10.1021/jp807972e (2009).

6 Liu, W. *et al.* Structural basis for allosteric regulation of GPCRs by sodium ions. *Science* **337**, 232-236, doi:10.1126/science.1219218 (2012).

7 Ballesteros, J. A., Weinstein H. Vol. 25 Ch. Methods Neuroscience, 366-428 (1995).

8 Adams, P. D. *et al.* PHENIX: a comprehensive Python-based system for macromolecular structure solution. *Acta Crystallogr D* **66**, 213-221, doi:10.1107/S0907444909052925 (2010).

9 Szekeres, P. G. & Traynor, J. R. Delta opioid modulation of the binding of guanosine-5'-O-(3-[35S]thio)triphosphate to NG108-15 cell membranes: characterization of agonist and inverse agonist effects. *J Pharmacol Exp Therap* **283**, 1276-1284 (1997).

10 Liu, J. G. & Prather, P. L. Chronic agonist treatment converts antagonists into inverse agonists at delta-opioid receptors. *J Pharmacol Exp Therap* **302**, 1070-1079, doi:10.1124/jpet.102.035964 (2002).